Reconstruction methods from hyperpolarized ^{13}C chemical shift imaging spiral 3D data: Comparison between direct summation and gridding method

Gibiino, F.; Positano, V.; Giovannetti, G.; Frijia, F.; Menichetti, L.; Ardenkjær-Larsen, Jan Henrik; Wiesinger, F.; Schulte, R.; De Marchi, D.; Lionetti, V.

Total number of authors:
14

Published in:
2012 9th IEEE International Symposium on Biomedical Imaging (ISBI)

Link to article, DOI:
10.1109/ISBI.2012.6235623

Publication date:
2012

Document Version
Publisher's PDF, also known as Version of record

RECONSTRUCTION METHODS FROM HYPERPOLARIZED ^{13}C CHEMICAL SHIFT IMAGING SPIRAL 3D DATA: COMPARISON BETWEEN DIRECT SUMMATION AND GRIDDING METHOD

F. Gibiino[a], V. Positano[b,c], G. Giovannetti[c], F. Frijia[b], L. Menichetti[c,b] J.H. Ardenkjaer-Larsen[d,e], F. Wiesinger[f], R. Schulte[f], D. De Marchi[b], V. Lionetti[g], G. Aquaro[b], M. Lombardi[b] , L. Landini[h,b,c] , M. F. Santarelli[c,b]

a: Dept of Energy and System Engineering - Univ. of Pisa, Italy; b: Fond. G. Monasterio CNR- Regione Toscana – Pisa, Italy; c: Inst. Clin. Phys., National Research Council – Pisa, Italy; d: GE Healthcare, Broendby, Denmark; e: Department of Electrical Engineering, The Technical University of Denmark, Kgs Lyngby, Denmark; f: GE Global Res., Munich, Germany; g: Lab. of Med. Sci., Inst. Life Sci., Scuola Superiore Sant'Anna – Pisa, Italy; h: Dept. of Inf. Eng.: EIT, Univ. of Pisa – Pisa, Italy.

ABSTRACT

Hyperpolarized ^{13}C chemical shift imaging (CSI) is a spectroscopy technique for magnetic resonance imaging. Due to the fast decay of the hyperpolarized tracer, acquisition speed represents a key issue. Spiral trajectories are usually exploited to fast fill the K-space. Several strategies have been proposed for CSI image reconstruction form spiral trajectories, but the performances in hyperpolarized ^{13}C CSI of these strategies have not been investigated. In hyperpolarized ^{13}C 3D CSI, some of the imaged metabolites may appear with very low signal, so reconstruction methods should keep SNR high to allow better viewing of metabolites' locations. In this study we compared the performances of Direct Summation (DS) and Gridding (GR) reconstruction methods. Methods were compared evaluating SNR on reconstructed images and reconstruction time. *In vivo* experimental data were obtained from medium-sized animals injected with hyperpolarized ^{13}C. DS obtained higher SNR for all metabolites of interest. On the other hand, GR was much faster. The study results may provide a useful indication on how to choose the appropriate reconstruction method for hyperpolarized ^{13}C *in vivo* data acquisition.

Index Terms— magnetic resonance imaging, non homogeneous MRI reconstruction, chemical shift imaging, *in vivo* hyperpolarized ^{13}C metabolism.

1. INTRODUCTION

Chemical Shift Imaging (CSI) is a magnetic resonance (MR) spectroscopy technique. CSI of hyperpolarized ^{13}C-labelled compounds represents a promising technique for *in vivo* metabolic studies. Hyperpolarization of ^{13}C increases the intensity of the ^{13}C MR signal by more than 10,000-fold [1]. The use of hyperpolarized ^{13}C-labeled pyruvate allows us to directly monitor the conversion of pyruvate to lactate, alanine and bicarbonate in both normal and malignant tissues [2]. Studies have been performed on cardiac metabolism after injection of [1-^{13}C]pyruvate [3][4]. Conversion of pyruvate in bicarbonate and lactate is the main factor characterizing aerobic and anaerobic behavior of the heart metabolism. However, whereas SNR is quite high for pyruvate, SNR for derivate metabolites is very low. A temporal sequence of 2D or 3D CSI must be acquired and processed when the metabolism of the heart is studied. High spatial and temporal resolution is needed to monitor the behavior of injected ^{13}C-labelled compound and its metabolites. A high amount of data needs to be processed, thus a reconstruction algorithm with high performance is required to obtain a high quality image in reasonable time. Spiral-based sequences are often used [5] to obtain a rapid acquisition. Non Cartesian trajectories can fill up the K-space with attractive performances. Spiral trajectories (Fig. 1) allow fast acquisition because gradients don't need to be switched on and off. Fewer samples can be acquired. Spirals oversample the center of K-space thus reducing movement

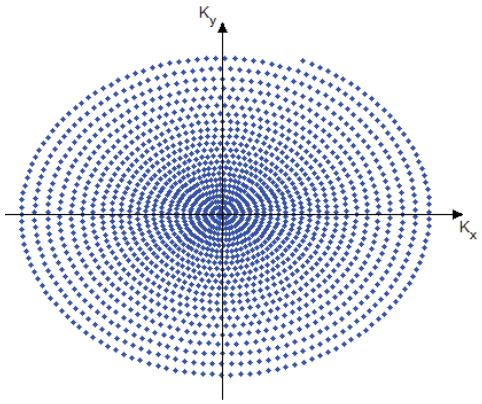

Fig. 1: Spiral trajectory. Sampling density is higher in the center than in the periphery of the K-space.

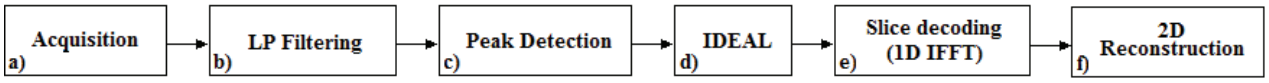

Fig. 2: Diagram of the 3D CSI data processing. a) Acquisition stage. b) Low-Pass filter to improve SNR of acquired data. c) Search for the resonance frequencies. Resonance frequency of the peaks in the spectrum can be achieved using matching pursuit. d) IDEAL implementation using a pseudo-inverse matrix. e) 1D IFFT along slice direction. f) 2D reconstruction of slices separately.

artifacts. However, non Cartesian sampling has disadvantages too. The Fast Fourier Transform (FFT) algorithm can't be directly used because it requires Cartesian input data. Thus the desired image in the space domain is achieved using reconstruction techniques.

We compared two reconstruction methods on cardiac spiral 3D CSI data. Data were acquired after injecting hyperpolarized [1-^{13}C]pyruvate on pigs. We refer to the first method as "Direct Summation" (DS). DS uses the definition of Inverse Discrete Fourier Transform (IDFT) [6]. We refer to the second method as "Gridding reconstruction" (GR). This second method uses an interpolation on Cartesian grid, followed by FFT algorithm [7]. The objective was to evaluate SNR and time performance of the two methods for pyruvate and its metabolic products using *in vivo* data.

2. MATERIALS AND METHODS

2.1. Theory

2.1.1. Direct Summation

Ideally, the general relationship between the space image $I(\vec{r})$ and the signal $s(\vec{k})$ acquired by the MR scanner is determined by the Fourier Transform:

$$I(\vec{r}) = \int s(\vec{k})\, e^{i2\pi\vec{k}\cdot\vec{r}}\, d\vec{k} \qquad (1)$$

Vector $\vec{r}$ represents space location and $\vec{k}$ represents frequency location in the K-space, for any dimension used.

In practice the acquisition has to be limited to a finite number (N_s) of samples. These samples are placed at frequency locations $\vec{k} = \vec{k}_n, n = 0 \dots N_s - 1$. The Fourier Transform in Eq. (1) needs to be discretized as follows:

$$I(\vec{r}) = \sum_{n=0}^{N_s-1} s(\vec{k}_n)\, e^{i2\pi\vec{k}_n\cdot\vec{r}}\, \Delta\vec{k}_n \qquad (2)$$

Term $\Delta\vec{k}_n$ represents a differential area dA and takes into account different densities of samples in the K-space. The higher the sampling density, the smaller the $\Delta\vec{k}_n$ associated to the sample. Sampling density depends on the trajectory chosen to fill the K-space. In practical cases $\Delta\vec{k}_n$ can be determined using the Voronoi diagram [6] as it was done in this work.

DS method can be described with a linear operation $I = ED \cdot s$. Vector I is the reconstructed image reshaped in one dimension. Vector s represents the N_s acquired data. Diagonal matrix D has $\Delta\vec{k}_n$ on its diagonal. E is the Fourier matrix and it's full. A generic element in matrix E is a complex exponential $E_{mn} = e^{i2\pi\vec{k}_n\cdot\vec{r}_m}$. The computational cost of the DS method equals a matrix-vector product.

2.1.2. Gridding reconstruction

Gridding reconstruction has the advantage of using FFT algorithm, which has low computational cost. Before using FFT, sampled data need to be interpolated on a Cartesian grid. The interpolation process is called 'gridding'.

Let us consider the 2D case for simplicity. We call M_s the sampled data. ρ is the density compensation function (DCF) and depends from the chosen trajectory [7]. DCF is proportional to the inverse of the $\Delta\vec{k}_n$ mentioned in section 2.1.1. We call C a chosen convolution kernel and III is the Cartesian grid where data are to be interpolated. Gridding process can thus be summarized as follows:

$$M_g = \left\{\left[\left(\frac{M_s}{\rho}\right)\otimes C\right]\cdot III\right\}\otimes^{-1} C \qquad (3)$$

M_g represents the gridded data and $\otimes$ is the convolution operator. Gridding is done with three main steps. The first step is a convolution between density compensated data and a chosen kernel C. The second step consists on re-sampling data onto a Cartesian grid. The last step is a scaling of the space image. Scaling corresponds to deconvolve ($\otimes^{-1}$) the obtained dataset with C in the frequency domain.

We chose shapes for kernel C and DCF as suggested by *Jackson et al*. [7]. We used Kaiser-Bessel (KB) window as C kernel, with parameters β=*8* and *w=4*. We calculated DCF with a convolution between the locations S of the trajectory samples and the convolution kernel C.

$$\rho = S \otimes C \qquad (4)$$

GR can be represented with a linear operation $M_g = TD \cdot M_s$. Matrix T is the interpolator. D is the diagonal matrix with $1/\rho$ on the diagonal. Kernel C can be defined to be non-zero on a very small number of points. This allows matrix T to be sparse and makes gridding very fast. Finally reconstruction can be obtained with the inverse FFT algorithm applied to M_g.

2.2. Measurements

We used 5 healthy male mini-pigs for animal experiments. Each experiment was performed on a 3T GE HDx MR scanner (GE Healthcare, Waukesha, WI) with a ^{13}C quadrature birdcage coil. A dose of 20 mL of 230 mM

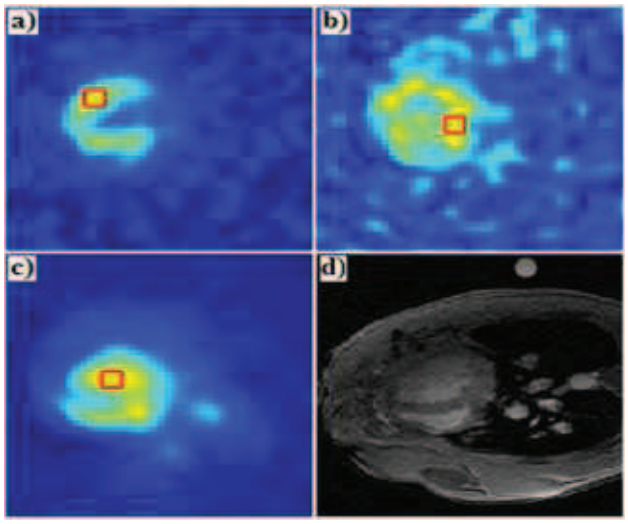

Fig. 4: Example of ROI selection on slice 32 of the first pig for SNR calculation: a) bicarbonate, b) lactate, c) pyruvate. Mean value was calculated in the red square. d) Corresponding anatomical image.

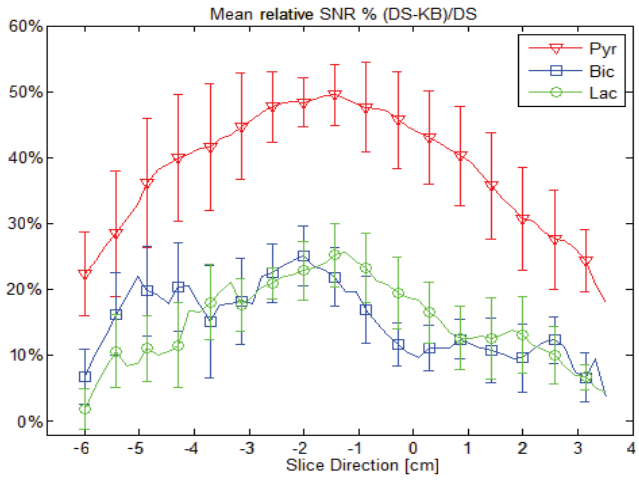

Fig. 3: Mean of the relative SNR over the pigs. Percentage values are plotted as function of the slice direction. Figure shows the mean value and the associated standard deviation for pyruvate, bicarbonate and lactate.

hyperpolarized [1-^{13}C]pyruvate was manually injected on the animal under sedation. [1-^{13}C]pyruvate hyperpolarization was obtained using a HyperSense DNP polarizer (OxfordInstruments, Oxford, UK) with subsequent dissolution.

Metabolic information covering the heart were obtained using a 3D IDEAL spiral CSI on a field of view (FOV) of 30×30 cm and slab thickness of 10cm. Acquisition started 20 seconds after the beginning of hyperpolarized [1-^{13}C]-pyruvate injection. We acquired a 3D volume of data and used a pulse-and-acquire sequence with a 2D spiral readout and phase encoding (PE) along the third dimension (z). 14 phase encodes along z direction were acquired. 11 echoes were acquired for each PE at different echo time (TE). We used a constant echo time shift of 0.9ms and FA=7°. We acquired 2048 samples for each echo, with a sample time-step of 16μs . For each PE an additional FID was acquired with high SNR for peak detection described in section 2.3.

Sampling along z direction was Cartesian. Thus we could obtain slices directly performing an 1D-FFT on z direction. We applied the reconstruction methods for 2D images separately for each slice.

2.3. Processing

The acquired raw data were processed as described by IDEAL method [8] before reconstruction.

Fig. 2 explains the process performed on each dataset of different pigs. Data were firstly low-pass-filtered to improve signal-to-noise-ratio (SNR). Secondly, resonance frequencies of the metabolites were identified. Resonance frequencies correspond to peaks in the acquired spectrum. IDEAL method needs precise estimate of resonance frequencies for accurate working. Resonance frequencies were detected using a matching pursuit (MP) algorithm [9]. MP iteratively looks for similarity between the signal and a model of the peak. When the highest matching is found, the model is subtracted to the signal and a search for another peak starts. Peak detection was done using FIDs with high SNR acquired for each slice. MP was applied on the FID with highest SNR. After frequency detection, the IDEAL method was applied. The pseudo-inverse matrix described in [8] was used to determine the data volume in the Fourier domain.

Finally reconstruction was done to achieve the desired image. Zero padding was used in reconstruction, thus obtaining a final volume of 64×64×64 points for each metabolite.

SNR was calculated for each slice of each metabolite in both DS and GR reconstruction methods. SNR was obtained as the ratio of mean signal to standard deviation of the noise. Mean signal was calculated in a rectangular ROI around the pixel with highest signal in the slice. Standard deviation of noise was estimated in a ROI at the periphery of the FOV. Fig. 3 shows an example of ROI selection for signal estimation of pyruvate, lactate and bicarbonate metabolites.

Reconstruction methods were compared by means of the relative SNR achieved. Relative SNR was calculated as the following ratio:

$$SNR_r(s,m,p) = \frac{SNR_{DS}(s,m,p) - SNR_{GR}(s,m,p)}{SNR_{DS}(s,m,p)} * 100\% \quad (5)$$

$SNR_r(s,m,p)$ stands for the relative SNR calculated for metabolite m, on slice s, in the dataset of pig p. SNR_{DS} is the SNR achieved in DS method. SNR_{GR} is the SNR achieved with GR method. A positive SNR_r means that DS achieves higher SNR than gridding method and vice versa.

We reported processing times of MATLAB implementations of reconstruction methods. We used a 2.61 GHz AMD Athlon(tm) 64 X2 Dual Core Processor and 1,50 Gb of RAM, with Windows 7OS.

3. RESULTS

We calculated the mean and the standard deviation of relative SNR over the pigs and for each metabolite. Fig. 4 shows the trend obtained for the mean as function of slice direction. Standard deviation was represented as vertical bars around the mean.

Afterwards we calculated the average over the slices for each metabolite (Tab. 1). Averages were weighted by the inverse of standard deviation. Associated uncertainties were calculated using the uncertainty propagation theory [10]. We assumed mean relative SNRs of different slices to be uncorrelated.

	Lactate	Bicarbonate	Pyruvate
Mean	13.5	12.2	38.2
Uncertainty	0.50	0.46	0.84

Tab. 1: Weighted average and uncertainty of mean relative SNR (percentage) for lactate, bicarbonate and pyruvate, calculated over the slices.

Positive relative SNR was achieved for all three metabolites. DS achieved an SNR about 13% better than GR for both lactate and bicarbonate. DS achieved an SNR about 38% better than GR for pyruvate.

Reconstruction time was evaluated (Tab. 2) averaging the reconstruction times for each slice and each metabolite.

Direct Summation	Gridding reconstruction
690±5 ms	10±5 ms

Tab. 2: average reconstruction time of a single slice of one metabolite, for the two reconstruction methods. Times are expressed in seconds unit.

GR method appears about two orders of magnitude faster than DS. Gridding reconstruction is faster because of the sparseness of interpolation matrix T, whereas E Fourier matrix is full.

4. CONCLUSION

The objective of this work was to compare DS and GR methods on hyperpolarized ^{13}C 3D CSI *in vivo* data.

We calculated the mean relative SNR over datasets of 5 medium-sized animals. DS method achieved an higher SNR than GR for all three metabolites. Thus DS method is better on hyperpolarized [1-^{13}C]pyruvate cardiac data.

We also evaluated the mean reconstruction time for both methods. GR was much faster than DS method.

Total reconstruction time for one pig dataset can be estimated multiplying the average reconstruction time in Tab. 2, times the number of metabolites, times the number of slices, times the number of 3D volumes.

The main targets of metabolic studies are bicarbonate and lactate. If the user can accept an image SNR degradation less than 13% GR method could be preferable because it achieves a faster reconstruction. This is especially intended for processing dynamic 3D CSI data (4D CSI) in order to study dynamic behavior of metabolites.

This work provides indication on how to choose a suitable reconstruction method for MR spectroscopy data. The novelty of the work is mainly the application of the two reconstruction methods to hyperpolarized ^{13}C CSI.

A possible extension of this work would be to compare other reconstruction methods besides the two herein studied. Other indicators for comparison could also be used together with relative SNR and processing time. Our evaluation of SNR should be coupled with an index that measures the fidelity of the reconstruction. A reference reconstructed image could be needed for this purpose.

5. REFERENCES

[1] J.H. Ardenkjaer-Larsen, B. Fridlund, A. Gram, G. Hansson, L. Hansson, M.H. Lerche, R. Servin, M. Thaning, K. Golman, "Increase in signal-to-noise ratio of >10,000 times in liquid-state NMR," *Proc. Natl. Acad. Sci. USA,* 100 (18), 10158–10163, 2003

[2] Golman K, in't Zandt R, Thaning M., "Real-time metabolic imaging," *Proc Natl Acad Sci USA,*103:11270–11275, 2006.

[3] F Frijia, F Wiesinger, MF Santarelli, V Positano, JH Ardenkjaer-Larsen, R Schulte, L Menichetti, G Giovannetti, G Bianchi, G Aquaro, V Lionetti, D De Marchi, A Flori, L Landini, FA Recchia, M Lombardi. "Detection of 3D Cardiac metabolism after injection of hyperpolarized [1-13C]pyruvate," *Journal of Cardiovascular Magnetic Resonance*, 13(Suppl 1):M2, 2011.

[4] MF. Santarelli, F. Frijia, L. Menichetti, V. Lionetti, A. Flori, G. Giovannetti, V. Positano, G. Aquaro, JH. Ardenkjaer-Larsen, M. Lombardi. "Cardiac metabolism with hyperpolarized [1-3C]pyruvate and chemical shift imaging at 3T," *European Heart Journal,* 32 (Abstract Supplement), 373, 2011.

[5] A.Z. Lau, A. P. Chen, N. R. Ghugre, V. Ramanan, W. W. Lam, K. A. Connelly, G. A. Wright, C. H. Cunningham. "Rapid Multislice Imaging of Hyperpolarized 13C Pyruvate and Bicarbonate in the heart," *Magn Res Med* 64(5): 1323–1331, 2010

[6] V. Rasche, R. Proksa, R. Sinkus, P. Börnert, H. Eggers, "Resampling of Data Between Arbitrary Grids Using Convolution Interpolation," *IEEE Trans. Med. Imag*, vol. 18, no. 5, 1999.

[7] J. I. Jackson, C. H. Meyer, D. G. Nishimura, and A. Macovski, "Selection of a convolution function for Fourier inversion using gridding," *IEEE Trans. Med. Imag.*, vol. 10, pp. 473–478, 1991.

[8] E.K. Brodsky, J.H. Holmes, H. Yu, S.B. Reeder, "Generalized *k*-Space Decomposition with Chemical Shift Correction for Non-Cartesian Water-Fat Imaging," *Magnetic Resonance in Medicine*, vol. 59, pp. 1151–1164, 2008.

[9] S. Mallat, Z. Zhang, "Matching Pursuit in a time-frequency dictionary," *IEEE Transactions on Signal Processing*, vol. 41, pp. 3397-3415, 1993.

[10] B.N. Taylor, C.E. Kuyatt, "Guidelines for Evaluating and Expressing the Uncertainty of NIST Measurement Results", NIST Technical Note 1297, 1994 Edition.